RSC Advances

ROYAL SOCIETY OF CHEMISTRY

www.rsc.org/advances

Journal Name

RSCPublishing

ARTICLE

POM-based inorganic-organic hybrid compounds: synthesis, structures, high-connected topologies and photodegradation of Organic dyes

Cite this: DOI: 10.1039/x0xx00000x

Received 00th January 2012,
Accepted 00th January 2012

DOI: 10.1039/x0xx00000x

www.rsc.org/

Xiao Li, Liu Yang, Chao Qin,* Fu-Hong Liu, Liang Zhao,* Kui-Zhan Shao and Zhong-Min Su*

Four new polyoxovanadate-based organic-inorganic hybrid materials $[MnV_2(bpp)_2O_6]$ (**1**), $[Ag_4V_4(bpp)_4O_{12}]\cdot 2H_2O$ (**2**) and $[M_3V_6(bpp)_4O_{18}\cdot 4H_2O]\cdot 2H_2O$ [M = Ni (**3**), Zn(**4**), bpp = 1,3-bis(4-pyridyl)propane] have been synthesized under hydrothermal conditions by self-assembly of transition metal salts, bpp ligands and ammonium metavanadate. Single-crystal X-ray diffraction analyses show that **1** reveals a three-dimensional framework, constructed from arrays of $\{V_4O_{12}\}$ rings covalently linked through metal-organic units, $\{Mn(C_{13}H_4N_2)_2\}$. Compound **2** is a eight-connected self-catenated metal-organic framework, based on bimetallic $\{Ag_4V_4O_{12}\}$ clusters as nodes. Compounds **3** and **4** are isostructural, both of them exhibit a intriguing 6,10-connected network. The structure of **4** , as an example, is based on single zinc atoms as six-connected nodes, while bimetallic $\{Zn_2V_6O_{18}\}$ clusters as ten-connected nodes, defining not only a new topology for three-periodic net but also the first 6,10-connected framework using heterometallic clusters as nodes. Furthermore, the thermal stabilities, photocatalytic activities of **1**-**4** have been discussed in detail.

Introduction

Organic-inorganic hybrid materials based on polyoxometalates (POMs) have attracted increasing interests due to their aesthetic architectures, intriguing topologies and potential applications in a variety of aspects, such as catalysis, electrochemistry, gas storage and magnetic materials, photochemistry, electromagnetic functional materials.[1] It is well known that the polyoxovanadates because of containing many $V_mO_n^{x-}$ subunits with rich oxygen atoms that can coordinate to various metal ions, have been regarded as suitable inorganic building blocks to form polyoxovanadate-based hybrid materials.[2-6] As one promising strategy namely using the polynuclear metal clusters as building blocks of constructing highly connected coordination frameworks, the polyoxovanadates can be promising building blocks for its advantages aforementioned.[7] Up to now, there are a handful of highly connected networks reported based on monometallic or heterometallic clusters.[8]

To date, a lot of N/O-donor organic ligands, including pyridine derivatives,[9] pyrazine derivatives,[10] imidazole derivatives,[11] carboxylic acids[12] and so on have been utilized to ligated with the vanadium resulting in multiple polyoxovanadate-based hybrid materials. Compared to the rigid bidentate 4,4-bipyridyl analogues, bpp is flexible dipyridyl ligands with different conformations, exhibiting lots of different N-to-N distances with respect to relative orientations of CH_2 groups and the pyridyl rings. The flexibility and conformation freedom of bpp ligands offer the possibility to meet the requirement of coordination geometries of different ions in the assembly process and construct charming frameworks with tailored properties and functions.[13] Therefore, we chose bpp as a bridging ligand to incorporate into the polyoxovanadate framework for producing unusual structures. As a result, four transition metal complex-based polyoxovanadate compounds $[MnV_2(bpp)_2O_6]$ (**1**), $[Ag_4V_4(bpp)_4O_{12}]\cdot 2H_2O$ (**2**) and $[M_3V_6(bpp)_4O_{18}\cdot 4H_2O]\cdot 2H_2O$ [M = Ni (**3**), Zn(**4**)] were obtained, which display 4,6-, 8- and 6,10-connected topologies with different three-dimensional structures. For the 6,10-connected topology network, it is not only a new topology as highly connected network but also the first 6,10-connected framework using heterometallic clusters as ten-connected nodes. The thermal stabilities, photocatalytic activities of **1**-**4** have been investigated.

Experimental section

Materials and methods

All reagents and solvents for syntheses were purchased from commercial sources and used as received without further purification. Elemental analyses (C, H, and N) were performed on a Perkin-Elmer 240C elemental analyzer. IR spectra were recorded in the range 400-4000 cm-1 on an Alpha Centaurt FT/IR spectrophotometer using KBr pellets. PXRD patterns were carried out with a Siemens D5005 diffractometer with Cu-*Kα* (λ = 1.5418Å) radiation in the range of 3-50° at 293 K. Thermogravimetric analyses (TGA) was conducted on Perkin-Elmer TG-7 analyzer heated from room temperature to 800 °C under nitrogen atmosphere at a rate of 10 °C min^{-1}. The UV/vis absorption spectra were examined on a Shimadzu UV-2550 spectrophotometer in the wavelength range of 200–800 nm. Inductively coupled plasma (ICP) analyses were conducted on a Leeman Laboratories Prodigy inductively coupled plasma−optical atomic emission spectrometry (ICP-AES) system.

Syntheses of compounds 1-4

Synthesis of $[MnV_2(bpp)_2O_6]$ (1). A mixture of $MnCl_2·4H_2O$ (0.040 g, 0.2 mmol), NH_4VO_3 (0.047 g, 0.4 mmol), bpp (0.030 g, 0.15 mmol) and H_2O (8 mL) was stirred for 30 min at room temperature. Then the mixture was sealed in a 15 mL Telfon reactor at 100 °C for 3 days. After slowly cooling to room temperature, orange block crystals of 1 were filtered and washed with deionized water. Yield: 42% (based on Mn). Anal. Calcd for $C_{26}H_{28}N_4MnO_6V_2$ (649.34): C 48.09, H 4.35, N 8.63, Mn 33.84, V 15.69; Found C 48.26, H 4.21, N 8.81, Mn 34.05, V 15.36. IR (KBr pellet, cm^{-1}): 3445 (s), 2930 (s), 1612 (m), 1504 (s), 1425 (s), 923 (w), 825 (w), 725 (w), 632 (w).

Synthesis of $[Ag_4V_4(bpp)_4O_{12}]·2H_2O$ (2). A mixture of $AgNO_3$ (0.034 g, 0.2 mmol), NH_4VO_3 (0.100 g, 0.8 mmol), bpp (0.030 g, 0.15 mmol) was dissolved in 8 mL distilled water at room temperature. Further the pH value of the mixture was adjusted to about 7.0 with 2mol L^{-1} NaOH. Then the mixture was stirred for 30 min at room temperature and was sealed in a 15 mL Telfon reactor at 100 °C for 3 days. After slowly cooling to room temperature, colourless block crystals of **2** were filtered and washed with deionized water. Yield: 38% (based on Ag). Anal. Calcd for $C_{52}H_{56}N_8Ag_4O_{15}V_4$ (1668.29): C 37.44, H 3.38, N 6.72, Ag 25.87, V 12.21; Found C 37.29, H 3.12, N 6.98, Ag 26.15, V 11.94. IR (KBr pellet, cm^{-1}): 3447 (s), 2931 (s), 1611 (m), 1501 (s), 1426 (s), 915 (s), 805 (m), 663 (s), 519 (w)..

Synthesis of $[Ni_3V_6(bpp)_4O_{18}·4H_2O]·2H_2O$ (3). A mixture of $NiCl_2·6H_2O$ (0.050 g, 0.2 mmol), NH_4VO_3 (0.047 g, 0.4 mmol), bpp (0.030 g, 0.15 mmol) was dissolved in 8 mL distilled water at room temperature. Then the pH value of the mixture was adjusted to about 3.0 with concentrated HNO_3. Then the mixture was stirred for 30 min at room temperature and was sealed in a 15 mL Telfon reactor at 100 °C for 3 days. After slowly cooling to room temperature, green blocks of crystals **3** were filtered and washed with deionized water. Yield: 65% (based on Ni). Anal. Calcd for $C_{52}H_{62}N_8Ni_3O_{24}V_6$ (1664.87): C 37.52, H 3.75, N 6.73, Ni 10.57, V 18.36; Found C 37.39, H 3.52, N 6.58, Ni 10.34, V 17.93. IR (KBr pellet, cm^{-1}): 3444 (s), 2930 (s), 1613 (m), 1493 (s), 1424 (s), 931 (s), 898 (m), 839 (s), 726 (w), 636 (w).

Synthesis of $[Zn_3V_6(bpp)_4O_{18}·4H_2O]·2H_2O$ (4). A mixture of $Zn(CH_3COO)_2·2H_2O$ (0.150 g, 0.7 mmol), NH_4VO_3 (0.047 g, 0.4 mmol), bpp (0.03 g, 0.15 mmol) and H_2O (8 mL) was stirred for 30 min at room temperature. Then the mixture was sealed in a 15 mL Telfon reactor at 100 **°C** for 3 days. After slowly cooling to room temperature, yellow block crystals of **4** were filtered and washed with deionized water. Yield: 55% (based on Zn). Anal. Calcd for $C_{52}H_{56}N_8Zn_3O_{24}V_6$ (1678.80): C 37.20, H 3.36, N 6.67, Zn 11.68, V 18.20; Found C 37.35, H 3.12, N 6.81, Zn 11.32, V 18.47. IR (KBr pellet, cm^{-1}): 3445 (s), 2931 (s), 1613 (w), 1504 (m), 1424 (m), 936 (s), 897 (m), 727 (w), 631 (m).

X-ray crystallography

Single-crystal X-ray diffraction data for **1-4** were collected on a Bruker SMART APEX II CCD diffractometer equipped with a graphite monochromator using Mo-*Kα* radiation (*λ* = 0.71073 Å) by using the Φ/*ω* scan technique at room temperature and there was no evidence of crystal decay during data collection. A multiscan technique was used to perform adsorption corrections. The crystal structures of 1-4 were solved using direct methods and refined using the full-matrix least-squares method on F^2 with anisotropic thermal parameters for all non-hydrogen atoms using the SHELXL-97 program.[14] Relevant crystal data and structure refinements for **1-4** are listed in Table 1. Selected bond lengths (Å) and angles (°) for **1-4** are given in Table S1.

Table 1. Crystallographic data for compounds 1–4

Compound	1	2	3	4
Chemical formula	$C_{26}H_{28}Mn_4O_6V_2$	$C_{52}H_{56}Ag_4N_8O_{15}V_4$	$C_{52}H_{62}N_8Ni_3O_{24}V_6$	$C_{52}H_{56}N_8O_{24}V_6Zn_3$
Formula weigh	649.34	1668.29	1664.87	1678.80
Crystal system	Tetragonal	Monoclinic	Monoclinic	Monoclinic
Space group	*I*4(1)/a	*P*2/n	*P*2(1)/n	*P*2(1)/n

a (Å)	21.5654(11)	12.382(3)	13.081(3)	13.1897(16)
b (Å)	21.5654(11)	9.697(2)	16.379(4)	16.438(2)
c (Å)	13.0149(8)	25.365(6)	15.407(4)	15.4725(19)
α (°)	90	90	90	90
β (°)	90	92.003(4)	102.368(5)	102.345(2)
γ (°)	90	90	90	90
V (Å^3)	6052.8(6)	3043.5(13)	3224.4(14)	3277.0(7)
Temperature (K)	293(2)	293(2)	293(2)	293(2)
Z	8	2	2	2
D_{calcd} (g · cm^{-3})	1.425	1.820	1.715	1.701
GOF on F^2	1.061	0.937	1.013	1.020
R_1 [$I > 2\sigma(I)$]^a	0.0393	0.0665	0.0376	0.0557
wR_2 [$I > 2\sigma(I)$]^b	0.1089	0.1537	0.0844	0.1431
$R_1{}^a$ (all data)	0.0551	0.1280	0.0632	0.0946
w$R_2{}^b$ (all data)	0.1173	0.1890	0.0968	0.1667
R_{int}	0.0502	0.0963	0.0460	0.0728

^{a} $R_1 = \sum||F_o| - |F_c||/\sum|F_o|$. ^{b} $wR_2 = |\sum w(|F_o|^2 - |F_c|^2)|/\sum|w(F_o^2)^2|^{1/2}$

Results and discussion

Description of crystal structures of $[MnV_2(bpp)_2O_6]$ (1).

Single X-ray diffraction analysis of **1** reveals that it crystallizes in the tetragonal group *I*4(1)/a. As shown in Fig. 1a, the asymmetric unit of **1** consists of a half Mn(II) ion, one bpp ligands and one V cation of a $\{V_4O_{12}\}$ ring. In the $\{V_4O_{12}\}$ ring, all the four vanadium atoms shows VO_4 tetrahedron coordination configuration, and each vanadium centre is coordinated with three bridging oxygen atoms (O_b) and one terminal oxygen atom (O_t). The V-O_t distance of 1.615(3) Å is slightly shorter than the V-O_b distances of 1.772(3) and 1.651(2) Å. The Mn1 ion is six-coordinated by four nitrogen atoms from four bpp ligands and two oxygen atoms from two adjacent $\{V_4O_{12}\}$ rings. The Mn-N bond lengths are 2.189(3) and 2.224(3) Å, and the Mn-O bond length is 1.995(2) Å, which are summarized in Table S1. Furthermore, all of the bpp ligands adopt a trans-gauche conformation.[15]

In **1**, the adjacent $\{V_4O_{12}\}$ rings are linked Mn ions to form netural bimetallic oxide layers $\{Mn_2V_4O_{12}\}$ (Fig.1b) with channels occupied by bpp ligands which cross-link the $\{Mn_2V_4O_{12}\}$ motifs to generate a three dimensional framework, shown in Fig 1c. In order to simplify the 3D framework of **1**, the Mn1 ion is regarded as a six-connected node and $\{V_4O_{12}\}$ rings can be considered as four-connected nodes. Thus, **1** exhibits a binodal (4,6)-connected 3D net with a $(4^4.5^5.6^6)_2(5^4.6^2)$ topology analysed by TOPOS software (Fig 1d).

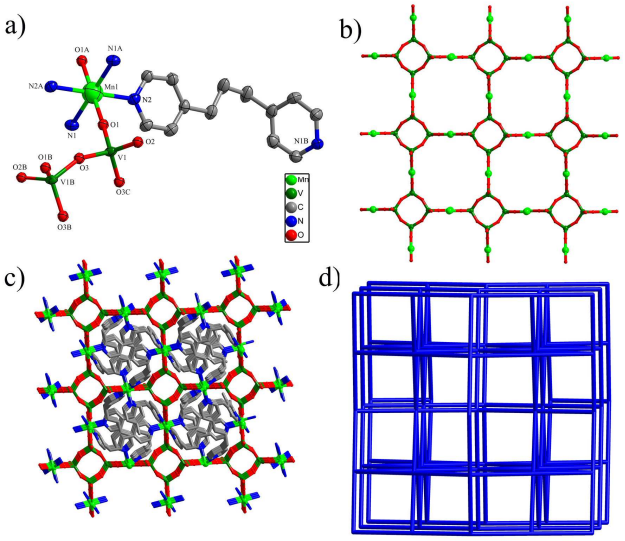

Fig. 1 (a) Mn(II) coordination environments of **1**. Symmetry codes: (A) –x + 1, −y + 2, −z; (B) –x + 3/2, − y + 2, z + 1/2; (C) x + 1/4, −y + 5/4, z + 1/4. (b) 2D layer of **1**. (c) 3D framework of **1**. (d) 3D binodal (4,6)-connected 3D net with a $(4^4.5^5.6^6)_2(5^4.6^2)$ topology of **1**. All hydrogen atoms are omitted for clarity.

Crystal structure of $[Ag_4V_4(bpp)_4O_{12}]\cdot 2H_2O$ (2). 2 contains neutral bimetallic $\{Ag_4V_4O_{12}\}$ clusters as nodes by Single-

crystal X-ray analysis, which consist of a central $\{V_4O_{12}\}^{4-}$ clusters decorated with four Ag units, as shown in the insert of Fig.2a. There are two crystallographically independent vanadium atoms in **2**, which shows similar distorted tetrahedral to 1.814(7) Å (Fig.2a). Tetrahedral and plane-traigonal coordination geometries of Ag ions are presented in Fig.2a. The Ag1 ion is coordinated by two nitrogen atoms from two bpp ligands and two terminal oxygen atoms from one $\{V_4O_{12}\}^{4-}$ anion, constructing a tetrahedral geometry. The Ag2 ion is ligated by two nitrogen atoms from two bpp ligands and one terminal oxygen atom from one $\{V_4O_{12}\}^{4-}$ anion to form a plane-traigonal geometry. The average Ag-O distance [2.636(3)Å] and Ag-N distance [2.222(8) Å] in the tetrahedron is longer than the corresponding values [2.371(8) Å and 2.145(9) Å] in the trigon. All the bpp ligands exhibit a trans-trans conformation with the present N-N distance is 9.718(0) to 10.191(4)Å. Fig.2b shows the Ag ions in adjacent $\{Ag_4V_4O_{12}\}$ clusters have Ag…Ag interactions with the short silver-silver contacts of 3.0767(19) and 3.2069(18) Å, which are shorter than the sum of the van der waals radii of two silver atoms (3.440(0) Å).[16] Every $\{Ag_4V_4O_{12}\}$ cluster is further connected to eight nearest neighbours through eight bpp ligands, thus resulting in a three-dimensional framework illustrated in Fig.2c.

From the viewpoint of the topology, each bimetallic $\{Ag_4V_4O_{12}\}$ cluster is surrounded by eight bridging bpp ligands, further connecting eight $\{Ag_4V_4O_{12}\}$ clusters with distances of 12.238(2) to 22.853(2) Å, defining an eight-connected node. In this bridging of parallel layers, the catenated four-membered shortest rings are observed at the intersection of the crossing of two-dimensional layers, therefore, resulting a single eight-connected self-catenated network (Fig.2d). The total Schlafli symbol of this net is $(4^{24}\cdot6^4)$. It is worth noting that the first self-catenated framework using heterometallic clusters as nodes was $[Cu_4(bpp)_4V_4O_{12}]\bullet3H_2O$ [bpp = 1,3-bis(4-pyridyl)propane] reported in 2007.[17]

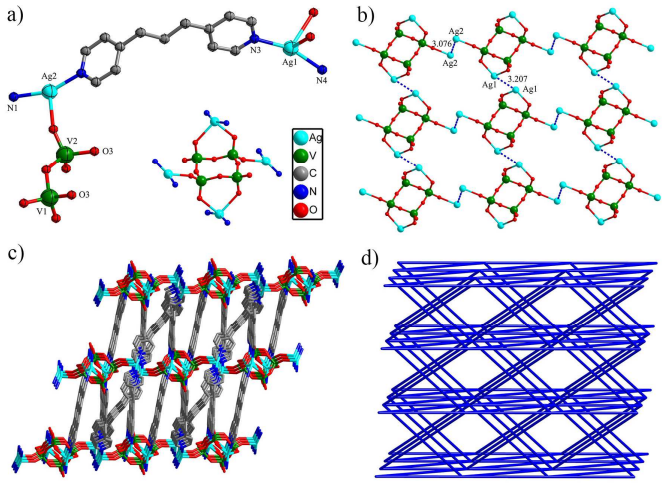

Fig. 2 (a) Ag(I) coordination environments of **2**. Symmetry codes: (A) –x, −y + 1, −z + 1; (b) The Ag…Ag interactions of adjacent $\{Ag_4V_4O_{12}\}$ clusters. (c) 3D framework of **2**. (d) 3D uninodal 8-connected networks with a $4^{24}\cdot6^4$ topology of **2**. All hydrogen atoms are omitted for clarity. The light blue, green, red and dark blue represent Silver, vanadium, oxygen and nitrogen atoms, respectively.

Crystal structure of $[Ni_3V_6(bpp)_4O_{18}\cdot4H_2O]\cdot2H_2O$ (3).

3-4 are isostructural, so the structural description of **3** is given as a representative example. Single-crystal X-ray diffraction analysis reveals that **3** crystallized in the monoclinic, space group *P*2(1)/n. As shown in Fig.3a, the asymmetric unit of **3** consists of one and a half Ni(II) ions, two bpp ligands and three vanadium atoms. All the vanadium atoms exhibit $\{VO_4\}$ tetrahedron coordination configuration, and each vanadium centre is coordinated with three bridging oxygen atoms (O_b) and one terminal oxygen atom (O_t). The V-O_b distances range from 1.650(2) to 1.809(2) Å are slightly longer than the values of V-O_t distances from 1.614(2) to 1.650(2) Å. Ni ions are six-coordinated showing octahedron geometry coordination but different coordination environments. The Ni1 ion is coordinated by two nitrogen atoms from two bpp ligands and four oxygen atoms from two vanadium tetrahedron and two water molecules. While Ni2 ion is ligated by four nitrogen atoms from four bpp ligands and two oxygen atoms from two vanadium tetrahedron. The Ni-N bond lengths are in the range of 2.077(2)-2.158(2) Å and the Ni-O distances vare from 2.042(2) to 2.113(3) Å (Table S1). All the bpp ligands show Trans-Gauche conformations

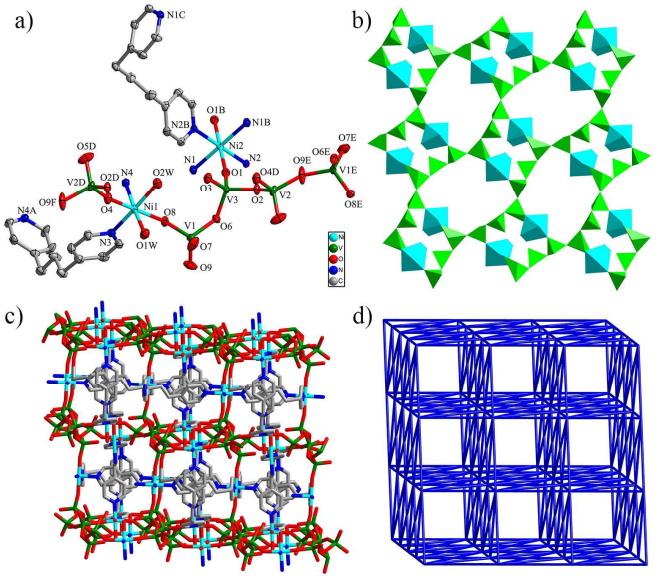

Fig. 3 (a) Ni(II) and coordination environments of **3**. Symmetry codes: (A) – x + 1/2, y – 1/2, −z + 3/2; (B) –x, − y + 1, − z + 1; (C) − x + 1/2, y + 1/2, − z + 3/2; (D) – x + 1, – y + 1, −z + 1; (E) – x + 1/2, y + 1/2, − z + 1/2; (F) x + 1/2, – y + 1/2, z + 1/2. (b) 2D inorganic layer of **3**. (c) 3D framework of **3**. (d) The binodal (6,10)-connected 3D net with a $(3^4\cdot4^8\cdot5^3)(3^8\cdot4^{20}\cdot5^{12}\cdot6^5)$ topology of **3**. All hydrogen atoms are omitted for clarity. The light blue, green, red and dark blue represent Nickel, vanadium, oxygen and nitrogen atoms, respectively.

with the N-N distance is 8.791(9) to 9.267(3) Å.

In **3**, two Ni1 ions and six vanadium atoms are bridged by eight bridging oxygen atoms to generate a bimetallic $\{Ni_2V_6O_{20}\}^{6-}$ clusters. Each $\{Ni_2V_6O_{20}\}^{6-}$ cluster links four neighbours by V_2-O_9-V_1 bridge to form 2D inorganic layers, given in Fig.3b. The 2D inorganic layers are further connected by the Ni2 ions through bridging oxygen atoms into a 3D framework (Fig.3c). From a topological point of view, each $\{Ni_2V_6O_{20}\}^{6-}$ cluster is surrounded by four bpp ligands, four neighbour $\{Ni_2V_6O_{20}\}^{6-}$ clusters and two Ni1 ions, which defines a bimetallic ten-connected node. Likewise, a Ni2 ion is surrounded by two $\{Ni_2V_6O_{20}\}^{6-}$ clusters and four bpp ligands, thus defining a six-connected node. Therefore, **3** presents a binodal (6,10)-connected 3D net with a point symbol of $(4^{13}\cdot6^2)(4^{36}\cdot6^9)$ in which each $\{Ni_2V_6O_{20}\}^{6-}$ cluster is linked to ten nearest-neighbours (eight $\{Ni_2V_6O_{20}\}^{6-}$ clusters and two Ni2 ions) and each Ni2 ion is linked to six nearest-neighbours (two $\{Ni_2V_6O_{20}\}^{6-}$ clusters and four Ni_2 ions) with distances of 6.594-13.882 Å(centre to centre), shown in Fig.3d.

To the best of our knowledge, only one (6,10)-connected structure has been reported up to now.[18] The example is $[Zn_7(trz)_6(pt)_4(H_2O)_2]$ (Htrz = 1,2,4-triazole, H_2pt= isophthalic acid) based on binuclear zinc cluster as six-connected nodes and pentanuclear zinc clusters as ten-connected nodes, meaning the first binodal (6,10)-connected metal-organic network with the topology of $(3^4\cdot4^8\cdot5^3)(3^8\cdot4^{20}\cdot5^{12}\cdot6^5)$.

Thermogravimetric analyses

To study the thermal stabilities of **1-4**, the thermogravimetric analyses were carried out under N_2 atmosphere from room temperature to 1000 °C with a heating rate of 10 °C min^{-1}. **1** shows a single weight loss step (Fig.S2). The loss step (180-240 °C for **1**) is corresponding to the decomposition of bpp ligands and $\{V_4O_{12}\}$ cluster. **2-4** exhibit three separate weight loss steps (Fig.S2). The first weight loss (120-200 °C for **2-4**) corresponds to the release of interstitial water molecules (found 3.21% for **2**, 6.54% for **3**, 6.47% for **4**; calcd. 4.11% for **2**, 5.35% for **3**, 6.04% for **4**). The second and third weight losses (300-800 °C for **2**, 270-800 °C for **3**-**4**) are attributed to the decomposition of bpp ligands and $\{Ag_4V_4O_{12}\}$ cluster for **2**, $\{M_2V_6O_{20}\}$ cluster for **3**-**4** [M=Ni(**3**),Zn(**4**)]. The remaining products should be MO (M= Mn, Ni, Zn), M_2O (M=Ag) and V_2O_5 (found. 38.93% for **1**, 49.64% for **2**, 46.25% for **3**, 47.13% for **4**; calcd. 38.46% for **1**, 48.27% for **2**, 5.82% for **3**, 46.55% for **4**).

Photocatalytic activity

It is well known that a wide range of polyoxovanadate-based compounds possess photocatalytic activities.[19] Herein, Methylene Blue (MB), a typical difficult-to-degrade dye contaminant model in waste water, was selected to evaluate the photocatalytic effectiveness of **1-4**. It is worth noting that **1-4** cannot be dissolved in aqueous solution, thus they are used as hetergenous catalysts. The photocatalytic reactions were performed as follows: 50mg of the catalyst (**1**-**4**) was dispersed in 300mL aqueous solution of MB (10mg L^{-1}) under stirring in the dark for 30min in order to rule out the effect of its absorption to the particle surfaces. Then the solution was exposed to UV light (125W) and kept continuous stirring. The samples of 5mL were taken out every 15min for UV measurement. The photodegradation process of MB without any photocatalyst was also performed for comparison.

Fig.4 and Fig.5 show the photocatalytic results of **1-4** in the MB solution. We can see that the absorption peaks of aqueous

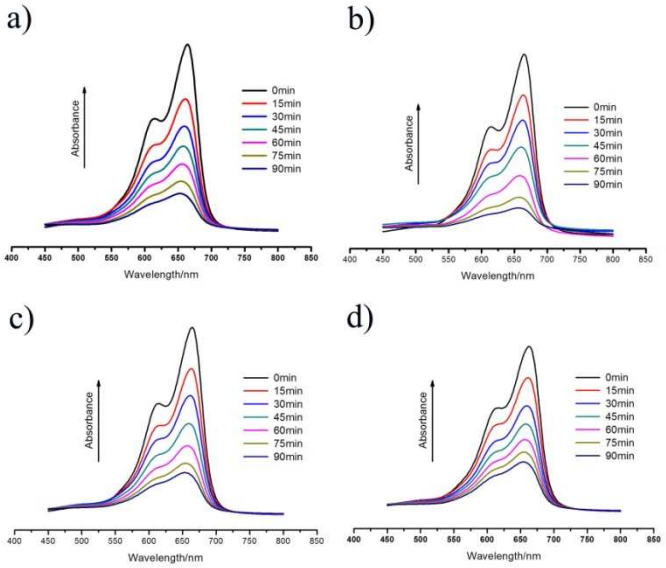

Figure 4. a)–d) UV/Vis absorption spectra of aqueous MB during the decomposition reaction under UV light irradiation in the presence of **1-4**, respectively.

MB in the presence of **1-4** dramatically decreased within 90min under UV irradiation from Fig.4. It is obvious that all the **1-4** show good photocatalytic activities for the degradation of MB. Furthermore, based on the plots of C_t/C_0 versus reaction time (Fig.5), it can be observed that the photocatalytic activities obviously increase from 25.8% to 79.9, 85.1, 77.4, 69.5% for **1-4**, respectively, after 90min of irradiation. The PXRD patterns of **1-4** simulated from single-crystal X-ray data, as-synthesized and after the photocatalytic reaction are shown in Fig.S2. The PXRD results reveal that **1-4** remain unchanged after the photocatalytic reaction, indicating that they are stable photocatalysts. Moreover, because **2** exhibits the highest catalytic activity in the degradation of MB under UV, it was chosen as a representative catalyst to investgate catalyst lifetime. In our initial experiment, the catalytic activity of **2** was maintained when it was recycled five times (Fig.S5). According to the related literatures,[20] the photocatalytic mechanisms may be deduced as follow: during the photocatalytic process, there is an electron transfer from the highest occupied molecular orbital (HOMO) to the lowest unoccupied molecular orbital (LUMO) which is produced from POM induced by UV light. The HOMO strongly needs an electron to return to its stable state. Therefore, one electron was abstracted from H_2O molecules, which was oxygenated into the •OH active species. Then

the ·OH radicals could cleave MB effectively to complete the photocatalytic process.

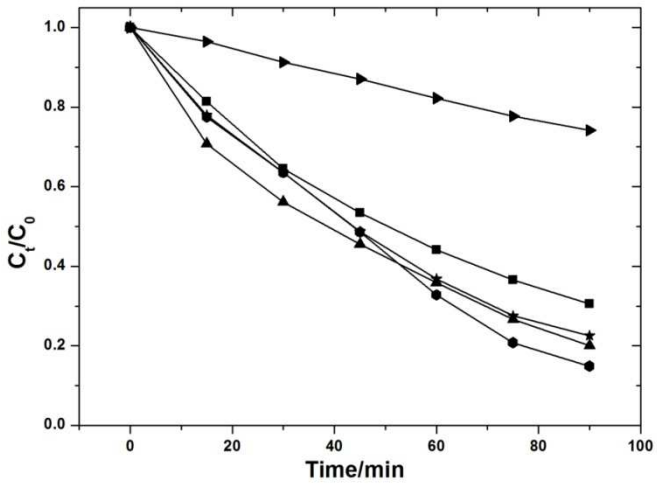

Figure 5. Plot of C_t/C_0 of MB versus irradiation time under UV light in the presence of **1–4** (**1** (▲); 2 (●); 3 (★), 4 (■); experiment in the absence of catalyst (►)).

Conclusions

Four new polyoxovanadate-based hybrid materials constructed from $\{V_4O_{12}\}$ cluster, $\{Ag_4V_4O_{12}\}$ cluster and $\{M_2V_6O_{20}\}$ cluster have been prepared under hydrothermal conditions, which all exhibit 3D frameworks with different topologies. **3-4** show a new complicated 6,10-connected topology. **2** shows good photocatalytic activity and selectivity for the degradation of MB. This work provides useful information of designing and constructing intriguing architectures of high dimensional and highly connected multifunctional polyoxovanandate-based hybrid materials.

Acknowledgements

This work was financially supported by the NSFC of China (No. 21471027, 21171033, 21131001, 21222105), National Key Basic Research Program of China (No. 2013CB834802), Changbai mountain scholars of Jilin Province.

Notes and references

Institute of Functional Material Chemistry, Faculty of Chemistry, Northeast Normal University, Changchun, 130024 Jilin, P. R. China. Email: zmsu@nenu.edu.cn

† Electronic Supplementary Information (ESI) available: the materials, synthesis methods, BVS, XRD, XPS, TGA, ESI-MS, UV-Vis diffuse reflectance spectra. (CCDC 1063206-1063209). For ESI and crystallographic data in CIF or other electronic format see DOI: 10.1039/b000000x/

1 (a) D. E. Katsoulis, *Chem. Rev.*, 1998, **98**, 359; (b) L. Carlucci, G. Ciani and D. M. Proserpio, *Coord. Chem. Rev.*, 2003, **246**, 247; (c) L.Cronin, *Chem. Soc. Rev.*, 2007, **36**, 105.; (d) J. Zhang, Y. F. Song, L. Cronin and T. B. Liu, *J. Am. Chem. Soc.*, 2008, **130**, 14408.; (e) D. L. Long, E. Burkholder and L. Cronin, *Chem. Soc. Rev.*, 2007, **36**, 105; (f) S. T. Zheng and G. Y. Yang, *Chem. Soc. Rev.*, 2012, **41**, 7623; (h) D. Y. Du, L. K. Yan, Z. M. Su, S. L. Li, Y. Q. Lan and E. B. Wang, *Coord. Chem. Rev.* , 2013, **257**, 702; (i) A. Dolbecq, E. Dumas, C. R. Mayer and P. Mialane, *Chem. Rev.* , 2010, **110**, 6009.

2 (a) V. Soghomonian, Q. Chen, R. C. Haushalter and J. Zubieta, *Angew. Chem. Int. Ed.*, 1995, **34**, 223; (b) C. L. Chen, A. M. Goforth, M. D. Smith, C. Y. Su, H. C, Z. Loye, *Angew. Chem. Int. Ed.*, 2005, **44**, 6673; (c) L. Luo and P. A. Maggard, *Cryst. Growth Des.*, 2013, **13**, 5282.

3 (a) R. F. de Luis, J. Orive, E. S. Larrea, M. K. Urtiaga and M. I. Arriortua, *Cryst. Growth Des.*, 2014, **14**, 658; (b) G. J. Cao, S. T. Zheng, W. H. Fang and G. Y. Yang, *Inorg. Chem. Commun.*, 2010, **13**, 834; (c) R. F. Luis, M. K. Urtiaga, J. L. Mesa, J. O. G. Segura, T. Rojo and M. I. Arriortua, *CrystEngComm.*, 2011, **13**, 6488.

4 (a) G. C. Ou, L. Jiang, X. L. Feng and T. B. Lu, *Dalton Trans.*, 2009, **38**, 71; (b) Y. Q. Lan, S. L. Li, Z. M. Su, K. Z. Shao, J. F. Ma, X. L. Wang and E. B. Wang, *Chem. Commun.*, 2008, **44**, 58; (c) J. Thomas, M. Agarwal, A. Ramanan, N. Chernova and M. S. Whittingham, *CrystEngComm.*, 2009, **11**, 625.

5 (a) Y. L. Teng, B. X. Dong, J. Peng, S. Y. Zhang, L. Chen, L. Song and J. Ge, *CrystEngComm.*, 2013, **15**, 2783; (b) Z. B. Zhang, Y. Xu, L. Zheng, D. R. Zhu and Y. Song, *CrystEngComm.*, 2011, **13**, 2191; (c) Y. Hu, F. Luo and F. F. Dong, *Chem. Commun.* , 2011, **47**, 761.

6 (a) X. L. Wang, C. H. Gong, J. W. Zhang, L. L. Hou, J. Luan and G. C. Liu, *CrystEngComm*, 2014,**16**, 7745.

7 （a）S. B. Li, W. Zhu, H. Y. Ma, H. J. Pang, H. Liu and T. T. Yu, *RSC. Adv.*, 2013, **3**, 9770; (b) X. L. Wang, C. Qin, E. B. Wang, Z. M. Su, Y. G. Li and L. Xu, *Angew. Chem., Int. Ed.* , 2006, **45**, 7411; (c) X. L. Wang, C. Qin, E. B. Wang and Z. M. Su, *Chem. Eur. J.* , 2006, **12**, 2680; (d) X. L. Wang, C. Qin, E. B. Wang, Z. M. Su, L. Xu and S. R. Batten, *Chem. Commun.*, 2005, 4789.; (e) J. Yang, B. Li, J. F. Ma, Y. Y. Liu and J. P. Zhang, *Chem. Commun.,* 2010, **46**, 8383; (f) Q. G. Zhai, J.P. Niu, S. N. Li, Y. C. Jiang, M. C. Hu and S. R. Batten, *CrystEngComm*., 2011, **13**, 4508.

8 (a) S. L. Cai, S. R. Zheng, Z. Z. Wen, J. Fan and W. G. Zhang, *Cryst. Growth Des.*, 2012, **12**, 5737; (b) K. H. He, W. C. Song, Y. W. Li, Y. Q. Chen and X. H. Bu, *Cryst. Growth Des.*, 2012, **12**, 1064; (c) X. L. Wang, C. Qin, Y. Q. Lan, K. Z. Shao, Z. M. Su and E. B. Wang, *Chem. Commun.*, 2009, 410.

9 (a) R. F. Luis, J. L. Mesa, M. K. Urtiaga, T. Rojo and M. I. Arriortua, *Eur. J. Inorg. Chem.*, 2009, **32**, 4786; (b) R. F. Luis, M. K. Urtiaga, J. L. Mesa, A. T. Aguayo, T. Rojo and M. I. Arriortua, *CrystEngComm.*, 2010, **12**, 1880.

10 (a) E. S. Larrea, J. L. Mesa, J. L. Pizarro, M. I. Arriortua and T. Rojo, *J. Solid State Chem.*, 2007, **180**, 1149; (b) J. Thomas, M. Agarwal, A. Ramanan, N. Chernov and M. S. Whittingham, *CrystEngComm.*, 2009, **11**, 625.

11 (a) Y. Q. Lan, S. L. Li, X. L. Wang, K. Z. Shao, D. Y. Du, Z. M. Su and E. B. Wang, *Chem. Eur. J.*, 2008, **14**, 9999; (b) X. L. Wang, B. K. Chen, G. C. Liu, H. Y. Lin, H. L. Hu and Y. Q. Chen, *J. Inorg.*

Organomet. Polym., 2009, **19**, 176. (c) J. X. Meng, Y. Lu, Y. G. Li, H. Fu and E. B. Wang, *Cryst. Growth Des.*, 2009, **9**, 4116.

12 (a) T. S-C. Law, H. H-Y. Sung and I. D. Williams, Inorg. Chem. Commun., 2000, 3, 420; (b) C. L. Pan, J. Q. Xu, K. X. Wang, X. B. Cui, L. Ye, Z. L. Lu, D. Q. Chu and T. G. Wang, Inorg. Chem. Commun., 2003, 6, 370.

13 (a) S. Wang, H. Xing, Y. Z. Li, J. F. Bai, Y. Pan, M. Scheer and X. Z. You, *Eur. J. Inorg. Chem.* 2006, 3041; (b) W. H. Zhang, J. P. Lang, Y. Zhang and B. F. Abrahams, *Cryst. Growth Des.,* 2008, **8**, 399; (c) J. Qian, H. Yoshikawa, J. F. Zhang, H. J. Zhao, K. Awaga, and C. Zhang, *Cryst. Growth Des.*, 2009, **9**, 5351; (d) P. Lin, W. Clegg, R. W. Harrington, R. A. Henderson, A. J. Fletcher, J. Bell and K. M. Thomas, *Inorg. Chem.*, 2006, **45**, 4284; (e) X. L. Wang, Y. F. Bi, B. K. Chen, H. Y. Lin, G. C. Liu, *Inorg. Chem.* 2008, **47**, 2442.

14 (a) G. M. Sheldrick. SHELXS97, A Program for the Solution of Crystal Structures from X-ray Data, University of GÖttingen, Germany, 1997; (b) G. M. Sheldrick. SHELXL97, A Program for the Refinement of Crystal Structures from X-ray Data , University of GÖttingen, Germany, GÖttingen, Germany, 1997.; (c) G. M. Sheldrick, *Acta Crystallogr. Sect. A*, 2008, **64**, 112.

15 (a) L. Carlucci, G. Ciani, D. M. Proserpiob and S. Rizzato, *CrystEngComm*., 2002, **4**, 121; (b) M.V. Marinho, M. I. Yoshida, K. J. Guedes, K. Krambrock, A. J. Bortoluzzi, M. Horner, F. C. Machado, W. M. Teles, *Inorg. Chem.*, 2004, **43**, 1539; (c) L. Pan, E. B. Woodlock, X. Wang, K. C. Lam, A. L. Rheingold, *Chem. Commun.*, 2001, 1762; (d) Y. M. Dai, E. Tang, J. F. Huang, Y. G. Yao, X. D. Huang, *J. Mol. Struct.*, 2009, 918, 183.

16 (a) Y.F. Qi, E. B. Wang, J. Li, Y. G. Li, *J. Solid. State.Chem.*, 2009, **182**, 2640.

17 (a) X. S. Qu, L. Xu, G. G. Gao, F. Y. Li, and Y. Y. Yang, *Inorg. Chem.*, 2007, **46**, 4775;

18 (a) J. Qin, C. Qin, C. X. Wang, H. Li, L. Cui, T. T. Li and X. L. Wang, *CrystEngComm.*, 2010, **12**, 4071.

19 (a) H. S. Lin and P. A. Maggard, *Inorg. Chem.*, 2008, **47**, 8051; (b) Y.
Hu, F. Luo and F. F. Dong, *Chem. Commun.*, 2011, **47**, 763; (c) Q. Wu, X. L. Hao, X. J. Feng, Y. H. Wang, Y. G. Li, E. B. Wang, X. Q. Zhu and X. H. Pan, *Inorg. Chem. Commun.*, 2012, **22**, 139; (d) C. C. Chen, W. Zhao, P. X. Lei, J. C. Zhao, N. Serpone, *Chem. Eur. J.*, 2004, **10**, 1956; (e) X. L. Hao, Y. Y. Ma, Y. H. Wang, L. Y. Xu, F. C. Liu, M. M. Zhang, Y. G. Li, *Chem. Asian. J.*, 2014, **9**, 819.

20 (a) Y. Q. Chen, G. R. Li, Y. K. Qu, Y. H. Zhang, K. H. He, Q. Gao and X. H. Bu, *Cryst. Growth Des*., 2013, **13**, 901; (b) J. W. Sun, M.T. Li, J. Q. Sha, P. F. Yan, C. Wang, S. X. Li and Y. Pan, CrystEngComm., 2013, 15, 10584; (c) X. L. Wang, J. Luan, F. F. Sui, H. Y. Lin, G. C. Liu and C. Xu, *Cryst. Growth Des.*, 2013, **13**, 3561.

Graphical Abstract

POM-based inorganic-organic hybrid compounds: synthesis, structures, high-connected topologies and photodegradation of Organic dyes

Xiao Li, Liu Yang, Chao Qin, Fu-Hong Liu, Liang Zhao,* Kui-Zhan Shao and Zhong-Min Su**

Institute of Functional Materials Chemistry, Key Laboratory of Polyoxometalate Science of Ministry of Education, Department of Chemistry, Northeast Normal University, Changchun 130024, China. E-mail: zmsu@nenu.edu.cn; qinc703@nenu.edu.cn; zhaol352@nenu.edu.cn

Four new polyoxovanadate-based organic-inorganic hybrid materials have been synthesized under hydrothermal conditions by self-assembly of transition metal salts, bpp ligands and ammonium metavanadate. The thermal stabilities and photocatalytic activities were also investigated.